Signal-Selective Time-Difference-of-Arrival Estimation for Passive Location of Man-Made Signal Sources in Highly Corruptive Environments, Part I: Theory and Method

William A. Gardner, *Fellow, IEEE,* and Chih-Kang Chen, *Member, IEEE*

Abstract—**For the problem of estimating time difference of arrival (TDOA) of radio waves impinging on a pair of antennas for the purpose of passively locating the source of a communications or telemetry signal in the presence of interfering signals and noise, a new class of signal-selective algorithms that is highly tolerant to interference and noise is introduced. In part I of this two-part paper, the background theory of cyclostationary signals is presented and applied to the design of various new TDOA methods. In part II, algorithmic implementations are described and their performance capabilities are assessed by analysis and simulation. By virtue of the fact that the multiple-signal resolution problem is essentially eliminated in many applications by the signal selectivity of the algorithms, two performance advantages are gained: 1) the practicality of source location based on time-difference measurements with relatively closely spaced antennas is substantially enhanced, and 2) the problem of sorting through multiple TDOA estimates, resulting from multiple interferers, for the estimate corresponding to a particular signal of interest is eliminated. These new algorithms exhibit their signal selectivity regardless of the extent of temporal, spectral, or spatial overlap among received signals. It is only required that the signal of interest have a known (or measurable) analog carrier frequency or digital keying rate that is distinct from those of all interfering signals. Yet the computational complexity of these algorithms is comparable to that of conventional generalized cross-correlation algorithms.**

I. Introduction

A. Background

The problem of passively locating the source of a propagating electromagnetic wave consisting of a man-made signal has a number of applications including direction finding for navigation by land, air, or sea, tracking of moving emitters for surveillance (e.g., for research, law enforcement, or national security), monitoring and locating illegal and/or hostile communicators (e.g., contraband, violators of communications regulations, or enemies in a battlefield), military reconnaissance and intelligence, and so on. Unlike active source-location systems, like radar, sonar, and lidar, which transmit signals and then process the received reflections from the objects to be located, passive systems simply process whatever signals are emitted from the object to be located.

In many of these passive source-location applications, the receivers in the source-location system are subject to a variety of types of electromagnetic interference and noise, including natural and manmade signals other than the signal of interest (SOI). These signals not of interest (SNOI) can severely degrade the performance of conventional source-location systems when they are present at the same time and also occupy the same spectral band as the SOI. This can be particularly problematic when the SOI is weak relative to the SNOI and/or noise. The problem is further exacerbated when the locations of the sources of the SNOI are unknown and/or close to that of the SOI.

The purpose of this paper is to present a new class of passive source-location methods that exploit an inherent signal property, called cyclostationarity, that is characteristic of man-made signals used for communications and telemetry to obtain substantial tolerance to all types of interference and noise (except for some interfering signals that are intentionally designed to exhibit the same cyclostationarity, e.g., in communication networks). Like most conventional methods (cf. [2]) that require some degree of tolerance to noise, the new methods are based on cross correlation of time-shifted measurements of data from multiple receivers. However, unlike conventional methods,[1] the new methods cross correlate frequency-shifted

Manuscript received July 19, 1990; revised April 5, 1991. This work was supported jointly by ESL, Inc., with partial matching support from the California State Micro Program, and the Army Research Office Sponsored by the United States Army Communications Electronics Command Center for Signals Warfare under Contract DAAL03-89-C-0035.

W. A. Gardner is with the Department of Electrical Engineering and Computer Science, University of California, Davis, CA 95616.

C.-K. Chen is with Silicon Engines, Palo Alto, CA 94303.

IEEE Log Number 9106570.

[1]Although cross-ambiguity methods (cf. [3]), which compensate for frequency difference of arrival due to Doppler effects, do cross correlate frequency-shifted data, the frequency shifts are relatively small since they correspond to Doppler shifts, whereas the frequency shifts used in the new methods are much larger than typical Doppler shifts and accomplish an entirely different task.

as well as time-shifted versions of the received data in order to exploit the unique cyclostationarity property of the SOI.

Within the general class of source-location methods that are based on cross-correlation measurements, there are two distinct subclasses: There are those methods that are designed for an array of closely spaced antenna elements on a single platform (e.g., a ship, aircraft, satellite, ground vehicle, or fixed ground station), for which the element spacing is typically less than half a wavelength for all signals received and phase-alignment methods for beam/null steering are employed; and there are those methods that are designed for two or three widely spaced antenna elements, each often (but not always) on a separate platform, where time-difference measurements are used to obtain location information. Whereas the former class of methods (often called direction finding methods) exploits phase differences (less than π rad in order to avoid ambiguities), from element to element, of relatively narrow-band signals (or wide-band signals decomposed into narrow-band components) to estimate angle of arrival, the latter class of methods (often called time-difference location methods) exploits relative time differences (the larger the better since root-mean-squared error of location is approximately inversely proportional to the separation between platforms) of preferably wide-band signals from platform to platform to estimate location (both angle of arrival and range). In practice, however, both methods can be applied to all bandwidths used in typical communications and telemetry systems.

The requirements on accuracy and spatial resolution capabilities of array-based methods become more stringent as the distance between each source to be located and the reception platform increases, since this decreases differences between angles of arrival. In contrast, the requirements on accuracy and temporal resolution capabilities of time-difference-of-arrival (TDOA)-based methods become less stringent as the separation between reception platforms increases, since this increases differences between times of arrival.

The need for high resolution arises primarily when (relatively) closely spaced multiple sources give rise to multiple received signals that cannot be separated by preprocessing (prior to processing for location). For instance, TDOA's of multiple signals that are not separated by more than the widths of their cross-correlation peaks (whose locations on the time-delay axis correspond to the TDOA's) usually cannot be resolved by conventional TDOA-based methods. To minimize this problem, the distance between platforms is typically made as large as is practically feasible so that the magnitudes of the TDOA's (which are proportional to the distance between platforms) will be as large as possible, thereby minimizing the overlap of adjacent peaks (whose widths depend only on the signal bandwidth—being inversely proportional—not on the distance between platforms). Specifically, in planar space the approximate minimum resolvable separation $\Delta\theta$ in angles of arrival (AOA) of two signals in the far field of the platform pair with approximately linear wavefronts can be derived as follows:

$$\frac{1}{B} < |D_1 - D_2| = \frac{L}{c}|\sin\theta_1 - \sin\theta_2|$$

$$= \frac{2L}{c}\left|\sin\left(\frac{\theta_1 - \theta_2}{2}\right)\right|\left|\cos\left(\frac{\theta_1 + \theta_2}{2}\right)\right|$$

where D_1 and D_2 are the two TDOA's in seconds, θ_1 and θ_2 are the corresponding AOA's in radians relative to broadside, L is the distance (in meters) between receivers, B is the signal bandwidth (in Hertz), and c is the speed of propagation (3×10^8 m/s). For $\Delta\theta \triangleq \theta_1 - \theta_2$ small, we can use $\sin(\Delta\theta/2) \cong \Delta\theta/2$ in this inequality to obtain

$$\Delta\theta_{\min} \cong \frac{c}{LB|\cos\theta|} \text{ rad},$$

where

$$\theta \triangleq (\theta_1 + \theta_2)/2.$$

For example, for $L = 3000$ m, $B = 1$ MHz, and $\theta = 60$ degrees, we obtain $\Delta\theta_{\min} \cong 12$ degrees. This relatively poor resolution becomes worse as either L or B is decreased.

The best performing array-based methods attempt to circumvent this resolution problem in locating multiple signal sources by simultaneously estimating multiple angles of arrival rather than individually estimating the angle of arrival of each signal (as commonly done by conventional beamformers and TDOA-based methods) [7]. Although the array-based methods offer the advantage of high spatial resolution (with respect to the spatial extent of the source-location system—the array size), and the ability to simultaneously locate a number of signals up to one less than the number of elements in the array, their complexity is typically much higher than that of the time-difference-of-arrival-based methods because of the need for measurement, storge, and usage of large amounts of array calibration data (the recently proposed ESPRIT method is an exception because of its special array design [4]), and because of the use of computationally intensive algorithms: the best performing algorithms require singular value decomposition of cross-correlation matrices of possibly high dimension, and/or require the solution of a multidimensional optimization problem [8], [9].

B. Overview

The new cyclostationarity-exploiting TDOA-based methods presented in this paper significantly alter this tradeoff between highly sophisticated high-resolution array-based methods and the relatively simple TDOA-based methods that require widely separated multiple platforms by eliminating the resolution-limitation problem for TDOA. That is, because the spectral correlations used make the new methods signal selective (in spite of tem-

poral and spectral overlap between the SOI and SNOI), they usually do not need to resolve multiple crosscorrelation peaks along the time-delay axis. As a result of this novel signal selectivity, the requirements on separation of platforms can be eased considerably. In fact, single-platform TDOA-based source-location systems in environments with SNOI become more practically feasible with the new methods. Also, the problem of deciding which peak among multiple cross-correlation peaks is associated with the SOI, and which with the SNOI, is eliminated. The only requirement of the new methods is that they must know a carrier frequency, or keying rate, or possibly some other cycle frequency associated with the cyclostationarity of the random SOI, although such cycle frequencies can be estimated using the same data to be used for TDOA estimation. These cycle frequencies are the frequency shifts used to obtain signal selectivity.

The objectives of this two-part paper are threefold: The first objective, which is met in part I, is to introduce a variety of new methods for signal-selective TDOA estimation; the second objective, which is met in part II [1], is to present the first quantitative results on a comparative performance study of some of these algorithms based on simulations. The results show that although all the algorithms tested do indeed offer the advantages described in this introduction, which accrue with signal selectivity, some algorithms are superior in the sense of yielding equal mean squared error (MSE) in the TDOA estimates with substantially less received data. In fact, some of these algorithms similarly outperform conventional TDOA algorithms even in the absence of SNOI, that is, when the only corruption to the SOI is receiver noise. The third objective, which is met in part I, is to introduce multiple-sensor-pair counterparts of some of these various TDOA-estimation methods. These counterparts, which accommodate multiple closely spaced sensors as well as widely spaced platforms and both wide-band and narrow-band signals, suggest that the dichotomy between the array-based direction finding problem and the time-difference location problem is not as strong as one might have thought.

Since the new methods derive their superior performance by exploiting a special statistical property shared by most communications and telemetry signals, the presentation begins in Section II by describing this special property, called cyclostationarity, in a suitable theoretical framework. This leads to a general cyclostationary model for the TDOA problem in Section III. Then in Section IV, each of a number of methods in the new class are derived and their principles of operation are explained. In part II, after a brief introduction in Section I, specific algorithms and practical considerations for digital implementation are presented and discussed in Section II. In Section III, the ability to eliminate the resolution-limitation problem is demonstrated qualitatively using the results of simulations, and in Section IV, the performance is quantitatively assessed by evaluating the MSE of TDOA estimates obtained from Monte Carlo simulations for a variety of environments and performance degrading conditions including single, multiple, narrow-band, and wide-band SNOI, weak SOI, SOI and SNOI with nearly the same cycle frequencies, and error in the algorithms' knowledge of the cycle frequency of the SOI. Conclusions are drawn in Section V.

II. Cyclostationarity and Spectral Correlation

Most signals encountered in communications and telemetry systems are appropriately modeled as cyclostationary time series rather than as stationary time series. This is a direct result of underlying periodicities in the time series due to periodic sampling, scanning, modulating, multiplexing, and coding operations employed in the transmitter. The cyclostationarity property can be used by receivers to obtain substantial tolerance to noise and interference for various signal processing tasks including TDOA estimation [10], [13]. The fundamentals of the spectral correlation theory of cyclostationary time-series are briefly surveyed in this section. This includes the limit cyclic mean, which is the characteristic property of what is called first-order periodicity, and the limit cyclic autocorrelation and limit cyclic spectrum, which are the characteristic properties of what is called second-order periodicity. The spectral correlation function, an alternative but equivalent characterization of second-order periodicity, is also described and its equivalence to the limit cyclic spectrum is explained. This material is a brief summary of the comprehensive treatment given in [10] that is provided for the reader's convenience. Somewhat more detailed surveys are given in [14], [15], [23].

A. Cyclic Autocorrelation and Cyclic Spectrum

Consider a time series $x(u)$ that contains an additive periodic component with period T_0. In order to extract the periodicity, a technique called synchronized averaging can be used. In this technique, for each location t, $2N + 1$ points are sampled from $x(u)$ with sampling interval T_0 and then summed to obtain the time-variant mean

$$M_x(t)_T \triangleq \frac{1}{2N+1} \sum_{n=-N}^{N} x(t + nT_0) \tag{1}$$

where $T \triangleq (2N + 1)T_0$ is the total length of the data segment over which averaging is carried out for each value of t. As the number of samples averaged increases without bound, randomness is completely averaged out and the limit time-variant mean is obtained

$$M_x(t) \triangleq \lim_{T\to\infty} M_x(t)_T = \lim_{N\to\infty} \frac{1}{2N+1} \sum_{n=-N}^{N} x(t + nT_0). \tag{2}$$

It can be shown from (2) that $M_x(t)$ is periodic with period T_0

$$M_x(t + T_0) = M_x(t) \tag{3}$$

and this limit function is, therefore, called the limit periodic mean. Applying the Fourier series expansion yields

$$M_x(t) = \sum_{m=-\infty}^{\infty} M_x^{m/T_0} e^{i2\pi mt/T_0} \tag{4a}$$

where the Fourier coefficients are given by

$$M_x^{m/T_0} \triangleq \frac{1}{T_0} \int_{-T_0/2}^{T_0/2} M_x(t) e^{-i2\pi mt/T_0}\, dt. \tag{4b}$$

Substituting (2) into (4b) produces the equivalence

$$M_x^{m/T_0} = \lim_{T\to\infty} \frac{1}{T} \int_{-T/2}^{T/2} x(t) e^{-i2\pi mt/T_0}\, dt \triangleq \langle x(t) e^{-i2\pi mt/T_0} \rangle \tag{5}$$

which is called the limit cyclic mean. Further substituting (5) into (4a) yields the synchronized averaging identity

$$M_x(t) = \lim_{N\to\infty} \frac{1}{(2N+1)} \sum_{n=-N}^{N} x(t + nT_0) = \sum_{m=-\infty}^{\infty} \lim_{T\to\infty} \frac{1}{T} \int_{-T/2}^{T/2} x(t+u) e^{-i2\pi mu/T_0}\, du. \tag{6}$$

For the situation in which $x(t)$ contains multiple incommensurate periodicities, the representation (4), (5) can be generalized to

$$M_x(t) \triangleq \sum_{\alpha} M_x^{\alpha} e^{i2\pi\alpha t} \tag{7a}$$

where

$$M_x^{\alpha} \triangleq \langle x(t) e^{-i2\pi\alpha t} \rangle \tag{7b}$$

with α representing all harmonics (integer multiples) of the fundamental frequencies of additive periodicities contained in $x(t)$.

We say that a time series contains first-order periodicity with frequency α if and only if M_x^{α} is not identically zero for some $\alpha \neq 0$. If the limit cyclic mean M_x^{α} exists in the temporal mean-square sense, then the time series exhibits a spectral line at frequency α with strength $|M_x^{\alpha}|^2$.

For a time series $x(t)$ that does not contain first-order periodicity (spectral lines), but does contain the more subtle form of periodicity called second-order periodicity, or cyclostationarity, synchronized averaging of the lag product can be used to extract the periodicity. Consider the time-variant autocorrelation

$$R_x(t, \tau)_T \triangleq \frac{1}{2N+1} \sum_{n=-N}^{N} x(t + \tau/2 + nT_0) \cdot x^*(t - \tau/2 + nT_0) \tag{8}$$

with $T \triangleq (2N+1)T_0$. Similar to (2), the randomness is averaged out when N increases without bound, and the limit time-variant autocorrelation, called the limit periodic autocorrelation, is obtained:

$$R_x(t, \tau) \triangleq \lim_{T\to\infty} R_x(t, \tau)_T = \lim_{N\to\infty} \frac{1}{2N+1} \sum_{n=-N}^{N} \cdot x(t + \tau/2 + nT_0) x^*(t - \tau/2 + nT_0). \tag{9}$$

By using the Fourier series expansion, (9) can be reexpressed as

$$R_x(t, \tau) = \sum_{m=-\infty}^{\infty} R_x^{m/T_0}(\tau) e^{i2\pi mt/T_0} \tag{10a}$$

where

$$R_x^{\alpha}(\tau) \triangleq \langle x(t + \tau/2) x^*(t - \tau/2) e^{-i2\pi\alpha t} \rangle \tag{10b}$$

which is called the limit cyclic autocorrelation, and the parameter α is called the cycle frequency. For $\alpha = 0$, (10b) is recognized as the conventional limit autocorrelation. The limit cyclic autocorrelation is a characteristic property of second-order periodicity, or cyclostationarity, in that $x(t)$ is said to contain second-order periodicity if and only if the limit cyclic autocorrelation is not identically zero for some nonzero cycle frequency α. When a time-series $x(t)$ contains multiple incommensurate second-order periodicities, (10a) generalizes to

$$R_x(t, \tau) \triangleq \sum_{\alpha} R_x^{\alpha}(\tau) e^{i2\pi\alpha t} \tag{11}$$

with α representing all harmonics of the fundamental frequencies of second-order periodicities contained in $x(t)$.

The limit cyclic spectrum is defined to be the Fourier transform of the limit cyclic autocorrelation

$$S_x^{\alpha}(f) \triangleq \int_{-\infty}^{\infty} R_x^{\alpha}(\tau) e^{-i2\pi f\tau}\, d\tau. \tag{12}$$

It follows from (10b) and (11) that for $\alpha = 0$ the limit cyclic spectrum becomes the conventional limit spectrum (or power spectral density).

For $x(t)$ real, $R_x^{\alpha}(\tau)$ has even symmetry in τ and $S_x^{\alpha}(f)$ has even symmetry in f. Also $R_x^{\alpha}(\tau)$ and $S_x^{\alpha}(f)$ have conjugate (Hermitian) symmetry in α. When $\alpha = 0$, we know that the conventional limit autocorrelation function has the property $R_x^0(0) \geq R_x^0(\tau)$. This property generalizes to $R_x^0(0) \geq R_x^{\alpha}(\tau)$.

The discrete-time counterparts of the limit cyclic autocorrelation and the limit cyclic spectrum are given by, respectively,

$$\tilde{R}_x^{\alpha}(kT_s) \triangleq \lim_{N\to\infty} \frac{1}{2N+1} \sum_{n=-N}^{N} x(nT_s + kT_s) x^*(nT_s) \cdot \exp[-i2\pi\alpha(n + k/2)T_s] \tag{13}$$

and

$$\tilde{S}_x^{\alpha}(f) \triangleq \sum_{k=-\infty}^{\infty} \tilde{R}_x^{\alpha}(kT_s) e^{-i2\pi fkT_s} \tag{14}$$

where T_s denotes the sampling period.

By applying the synchronized average identity (6) to the lag product of $x(t)$, the relationship between the limit cyclic autocorrelations for $x(t)$ and $\{x(nT_s)\}$ is found to be

$$\tilde{R}_x^{\alpha}(kT_s) = \sum_{m=-\infty}^{\infty} R_x^{\alpha+m/T_s}(kT_s) e^{i\pi mk}. \tag{15}$$

By substituting (15) into (14), we obtain the relationship between the two spectral correlation functions:

$$\tilde{S}_x^\alpha(f) = \frac{1}{T_s} \sum_{n,m=-\infty}^{\infty} S_x^{\alpha+m/T_s}\left(f - \frac{m}{2T_s} - \frac{n}{T_s}\right). \quad (16)$$

It can be seen that $\tilde{S}_x^\alpha(f)$ is a periodic function of f and α with periods of $1/T_s$ and $2/T_s$, respectively; that is,

$$\tilde{S}_x^\alpha\left(f + \frac{n}{T_s}\right) = \tilde{S}_x^\alpha(f) \quad (17a)$$

and

$$\tilde{S}_x^{\alpha+2n/T_s}(f) = \tilde{S}_x^\alpha(f). \quad (17b)$$

In addition, $\tilde{S}_x^\alpha(f)$ is jointly periodic in f and α; that is,

$$\tilde{S}_x^{\alpha+n/T_s}\left(f - \frac{n}{2T_s}\right) = \tilde{S}_x^\alpha(f) \quad (17c)$$

for all integers n.

B. Spectral and Temporal Coherence

An alternative way to characterize second-order periodicity is in terms of spectral correlation. Consider the time-variant finite-time complex spectrum of $x(t)$

$$X_T(t, f) \triangleq \int_{t-T/2}^{t+T/2} x(u)\, e^{-i2\pi fu}\, du \quad (18)$$

which is a measurement of temporally local frequency content of $x(t)$ in the interval $[t - T/2, t + T/2]$ with spectral resolution width $1/T$. The complex spectrum $X_T(t, f)$ is shifted in frequency from f to $f + \alpha/2$ and $f - \alpha/2$, and the bandwidth-normalized temporal correlation of the two shifted time-variant complex spectra is measured,

$$S_{xT}^\alpha(t, f)_{\Delta t} \triangleq \frac{1}{\Delta t} \int_{t-\Delta t/2}^{t+\Delta t/2} \frac{1}{T} X_T(s, f + \alpha/2) \cdot X_T^*(s, f - \alpha/2)\, ds. \quad (19)$$

Then letting $\Delta t \to \infty$ to remove all randomness, (16) becomes (using (18))

$$\begin{aligned}
&\lim_{\Delta t\to\infty} S_{xT}^\alpha(t, f)_{\Delta t} \\
&= \frac{1}{T} \int_{-T/2}^{T/2}\int \left[\lim_{\Delta t\to\infty} \frac{1}{\Delta t} \int_{t-\Delta t/2}^{t+\Delta t/2} x(s + u) \cdot x^*(s + v) e^{-i2\pi\alpha s}\, ds\right] e^{-i2\pi f(u-v)} e^{-i\pi\alpha(u+v)}\, du\, dv \\
&= \frac{1}{T} \int_{-T/2}^{T/2}\int R_x^\alpha(u - v) e^{-i2\pi f(u-v)}\, du\, dv \\
&= \int_{-T/2}^{T/2} R_x^\alpha(\tau)\left[1 - \frac{|\tau|}{T}\right] e^{-i2\pi f\tau}\, d\tau. \quad (20)
\end{aligned}$$

Finally, letting $T \to \infty$ to obtain unlimited spectral resolution results in

$$\begin{aligned}
&\lim_{T\to\infty}\lim_{\Delta t\to\infty} S_{xT}^\alpha(t, f)_{\Delta t} \\
&= \lim_{T\to\infty} \int_{-T/2}^{T/2} R_x^\alpha(\tau)\left[1 - \frac{|\tau|}{T}\right] e^{-i2\pi f\tau}\, d\tau \\
&= \lim_{T\to\infty} \int_{-T/2}^{T/2} R_x^\alpha(\tau) e^{-i2\pi f\tau}\, d\tau \\
&= S_x^\alpha(f). \quad (21)
\end{aligned}$$

Thus, it is seen from (21) that the limit cycle spectrum defined by (10b) and (11) can be obtained by first measuring the correlation of two spectral components at frequencies $f + \alpha/2$ and $f - \alpha/2$ and then idealizing the measurement by letting $\Delta t \to \infty$ followed by letting $T \to \infty$. Consequently, the limit cyclic spectrum is called the spectral correlation function.

The spectral correlation function can be reinterpreted as the conventional cross spectral density for the pair of time series

$$u(t) \triangleq x(t) e^{-i\pi\alpha t} \quad (22a)$$

$$v(t) \triangleq x(t) e^{i\pi\alpha t} \quad (22b)$$

obtained by frequency shifting $x(t)$. Since

$$R_{uv}^0(\tau) \triangleq \langle u(t + \tau/2) v^*(t - \tau/2)\rangle = R_x^\alpha(\tau) \quad (23)$$

then,

$$S_{uv}^0(f) \triangleq \int_{-\infty}^{\infty} R_{uv}^0(\tau) e^{-i2\pi f\tau}\, d\tau = S_x^\alpha(f). \quad (24)$$

In other words, the density of correlation between spectral components at frequency f in $u(t)$ and $v(t)$ is identical to the density of correlation between spectral components at frequencies $f + \alpha/2$ and $f - \alpha/2$ in $x(t)$. Also, since it follows from (22) that

$$S_u^0(f) = S_x^0(f + \alpha/2) \quad (25a)$$

$$S_v^0(f) = S_x^0(f - \alpha/2) \quad (25b)$$

then the normalized cross-spectral density

$$C_{uv}(f) \triangleq \frac{S_{uv}^0(f)}{[S_u^0(f) S_v^0(f)]^{1/2}} \quad (26)$$

which is the spectral cross-coherence function, is identical to

$$C_{uv}(f) = \frac{S_x^\alpha(f)}{[S_x^0(f + \alpha/2) S_x^0(f - \alpha/2)]^{1/2}} \triangleq C_x^\alpha(f) \quad (27)$$

which is called the spectral autocoherence function [10].

The spectral autocoherence function is a frequency decomposed correlation coefficient (assuming that $m_x^{f\pm\alpha} = 0$ so that the correlation $S_x^\alpha(f)$ is a covariance) for the frequency-shifted versions (22) of $x(t)$. Thus, it has the

property $|C_x^\alpha(f)| \leq 1$, which is held by all correlation coefficients. Analogously, the quantity

$$K_x(\tau) \triangleq \frac{R_x^0(\tau)}{R_x^0(0)} \tag{28}$$

which is called the temporal autocoherence function, is the correlation coefficient (assuming that $m_x^0 = 0$) for the time-shifted versions

$$u'(t) \triangleq x(t + \tau/2) \tag{29a}$$

$$v'(t) \triangleq x(t - \tau/2) \tag{29b}$$

of $x(t)$. Similarly, the more general temporal/spectral autocoherence function[2]

$$K_x^\alpha(\tau) \triangleq \frac{R_x^\alpha(\tau)}{R_x^0(0)} \tag{30}$$

is the correlation coefficient (assuming $m_x^\alpha = 0$) for the time- and frequency-shifted versions

$$u''(t) \triangleq x(t + \tau/2)e^{-i\pi\alpha t} \tag{31a}$$

$$v''(t) \triangleq x(t - \tau/2)e^{+i\pi\alpha t} \tag{31b}$$

of $x(t)$. The Fourier transform of the unnormalized version $R_x^\alpha(\tau)$ of $K_x^\alpha(\tau)$ is the unnormalized spectral autocoherence function $S_x^\alpha(f)$.

For a pair of time-series $x(t)$ and $y(t)$, the natural generalization of $K_x^\alpha(\tau)$ is given by

$$K_{yx}^\alpha(\tau) = \frac{R_{yx}^\alpha(\tau)}{[R_y^0(0)R_x^0(0)]^{1/2}} \tag{32}$$

and the natural generalization of $C_x^\alpha(f)$ is given by

$$C_{yx}^\alpha(f) = \frac{S_{yx}^\alpha(f)}{[S_y^0(f + \alpha/2)S_x^0(f - \alpha/2)]^{1/2}} \tag{33}$$

where

$$R_{yx}^\alpha(\tau) \triangleq \langle y(t + \tau/2)x^*(t - \tau/2)e^{-i2\pi\alpha t} \rangle \tag{34}$$

and

$$S_{yx}^\alpha(f) \triangleq \int_{-\infty}^{\infty} R_{yx}^\alpha(\tau)e^{-i2\pi f\tau}\, d\tau \tag{35}$$

or

$$S_{yx}^\alpha(f) \triangleq \lim_{T\to\infty} \lim_{\Delta t\to\infty} S_{yxT}^\alpha(t, f)_{\Delta t} \tag{36}$$

in which

$$S_{yxT}^\alpha(t, f)_{\Delta t} \triangleq \frac{1}{\Delta t} \int_{t-\Delta t/2}^{t+\Delta t/2} \frac{1}{T} Y_T(s, f + \alpha/2) \cdot X_T^*(s, f - \alpha/2)\, ds. \tag{37}$$

Conventional methods of TDOA estimation, some of which are described, for example, in [2], [11], and [16], are based on the unnormalized temporal cross coherence function $R_{yx}^0(\tau)$ and its Fourier transform $S_{yx}^0(f)$. The new methods of TDOA estimation presented in Section IV are based on the unnormalized temporal/spectral cross coherence function $R_{yx}^\alpha(\tau)$ and its Fourier transform $S_{yx}^\alpha(f)$, the unnormalized spectral cross coherence function. Examples of the functions $R_{yx}^\alpha(\tau)$ and $S_{yx}^\alpha(f)$ for numerous types of communication/telemetry signals are described in [10], [13], [17], [18]. One such example is given in the Appendix. As explained in the references, typical cycle frequencies α in these signals include the keying rate, $\alpha = \alpha_k$, and its harmonics in keyed digital systems, such as amplitude-, phase-, and frequency-shifted keying (ASK, PSK, and FSK), and the doubled carrier frequency, $\alpha = 2f_c$, in continuous-wave analog systems, such as amplitude, phase, and frequency modulation (AM, PM, and FM), as well as sums and differences of these cycle frequencies in digital carrier-modulated systems such as ASK, PSK, and FSK.

Because of the current and growing popularity of PSK in both communications and telemetry systems, the simulations in Part II of this paper focus on this type of signal for the SOI, but consider both PSK and AM for the SNOI. Since carrier frequencies used in the transmitter are easily changed, they can be more difficult for an unintended receiver to have knowledge of them. Consequently, only the keying rate in the PSK SOI is used in the simulations presented in Part II. Nevertheless, it is pointed out that for signals that do possess the cycle frequency $\alpha = 2f_c$, the spectral correlation at $\alpha = 2f_c$ is typically stronger than that at $\alpha = \alpha_k$ and, consequently, the performance of TDOA estimators that exploit $\alpha = 2f_c$ is typically superior. It also should be clarified that when complex data $x(t)$ is used, and α equal to or associated with a carrier frequency is used, then the conjugate cyclic correlations, for which the conjugate in (10b) and (34) is removed, must be used. As a consequence of this, the conjugates in (19) and (37) must be removed from the second factor and the argument $f - \alpha/2$ in this factor must be changed to $\alpha/2 - f$ [10].

III. Cyclostationary Model for TDOA

Before proceeding to the introduction of the cyclostationarity-exploiting methods for estimating TDOA, let us first determine the general form of the functions $R_{yx}^\alpha(\tau)$ and $S_{yx}^\alpha(f)$, as well as $R_x^\alpha(\tau)$, $R_y^\alpha(\tau)$, $S_x^\alpha(f)$, and $S_y^\alpha(f)$, for the particular model of $x(t)$ and $y(t)$ that describes the data received from a pair of antenna elements.

A signal (SOI) radiating from a remote source, propagating through a nondispersive medium, and impinging on two spatially separated antenna elements, together with interfering signals (SNOI), and received in the presence of receiver (including antenna) noise, can be modeled as

$$x(t) = s(t) + n(t) \tag{38a}$$

$$y(t) = As(t - D) + m(t) \tag{38b}$$

[2]Although it would seem to be consistent to call $R_x^\alpha(0)/R_x^0(0)$ the spectral autocoherence function, this term is reserved for (27).

where $s(t)$ is the SOI, $n(t)$ and $m(t)$ are the SNOI, including noise, D is the TDOA to be estimated using measurements $x(t)$ and $y(t)$, and A represents magnitude (and phase for complex data) mismatch between receivers. In this ideal model all signal distortion due to the propagation channels and the sensors is assumed to be negligible or to be matched (i.e., matched sensors and matched channels). The effects of mismatch here are described in part II [1]. It is also assumed that $s(t)$, $n(t)$, and $m(t)$ have zero-mean (time average) values, and that $s(t)$ is statistically independent (over time) of $n(t)$ and $m(t)$. However, since $n(t)$ and $m(t)$ can contain the same interfering signals (with different times of arrival), as well as independent receiver noise, then they can be statistically dependent. It follows that the limit cyclic cross correlation and autocorrelations are given by

$$R_{yx}^{\alpha}(\tau) = AR_s^{\alpha}(\tau - D)e^{-i\pi\alpha D} + R_{mn}^{\alpha}(\tau) \quad (39a)$$

$$R_x^{\alpha}(\tau) = R_s^{\alpha}(\tau) + R_n^{\alpha}(\tau) \quad (39b)$$

$$R_y^{\alpha}(\tau) = |A|^2 R_s^{\alpha}(\tau)e^{-i2\pi\alpha D} + R_m^{\alpha}(\tau). \quad (39c)$$

The limit cyclic cross spectrum and autospectra can be obtained by Fourier transforming (39), and are given by

$$S_{yx}^{\alpha}(f) = AS_s^{\alpha}(f)e^{-i2\pi(f+\alpha/2)D} + S_{mn}^{\alpha}(f) \quad (40a)$$

$$S_x^{\alpha}(f) = S_s^{\alpha}(f) + S_n^{\alpha}(f) \quad (40b)$$

$$S_y^{\alpha}(f) = |A|^2 S_s^{\alpha}(f)e^{-i2\pi\alpha D} + S_m^{\alpha}(f). \quad (40c)$$

Although these ideal (infinite-time average) measurements contain the TDOA parameter D to be estimated, the parts of these measurements that contain the parameter D, namely, those dependent on the SOI $s(t)$, are masked by the parts due to the SNOI $n(t)$ and $m(t)$. As a result, when the SNOI are both temporally and spectrally coincident with the SOI (and knowledge required to do spatial filtering to reject the interfering signals in $n(t)$ and $m(t)$ prior to recording $x(t)$ and $y(t)$ is not available), then conventional methods which use these measurements with only $\alpha = 0$ cannot avoid the resolution-limitation problem described in Section I. Furthermore, even if the individual cross-correlation peaks due to the SOI and SNOI can be resolved, the conventional methods still have to determine which of the multiple peaks is due to the SOI and which are due to the SNOI.

In contrast to this difficult situation, if the SOI exhibits a cycle frequency α not shared by any of the SNOI (this is usually the case since keying rates and carrier frequencies of a SOI are rarely the same as those of the SNOI even though signals reside in the same band), then by using this value of α in the measurements (39), (40), we obtain (ideally, for infinite averaging time)

$$R_n^{\alpha}(\tau) \equiv R_m^{\alpha}(\tau) \equiv R_{mn}^{\alpha}(\tau) \equiv 0 \quad (41)$$

and, therefore,

$$S_n^{\alpha}(f) \equiv S_m^{\alpha}(f) \equiv S_{mn}^{\alpha}(f) \equiv 0. \quad (42)$$

This is the means by which we obtain signal selectivity in our measurements. Using (41) and (42), (39) and (40) reduce to

$$R_{yx}^{\alpha}(\tau) = AR_s^{\alpha}(\tau - D)e^{-i\pi\alpha D} \quad (43a)$$

$$R_x^{\alpha}(\tau) = R_s^{\alpha}(\tau) \quad (43b)$$

$$R_y^{\alpha}(\tau) = |A|^2 R_s^{\alpha}(\tau)e^{-i2\pi\alpha D} \quad (43c)$$

and

$$S_{yx}^{\alpha}(f) = AS_s^{\alpha}(f)e^{-i2\pi(f+\alpha/2)D} \quad (44a)$$

$$S_x^{\alpha}(f) = S_s^{\alpha}(f) \quad (44b)$$

$$S_y^{\alpha}(f) = |A|^2 S_s^{\alpha}(f)e^{-i2\pi\alpha D}. \quad (44c)$$

These ideal measurements are the same as those we would obtain directly from the idealized SNOI-free model

$$x(t) = s(t) \quad (45a)$$

$$y(t) = As(t - D). \quad (45b)$$

Observe that these same results hold true when there are multiple SOI in the environment, each exhibiting a distinct cycle frequency α. In practice, if there are signals of potential interest whose cycle frequencies α are not known in advance, these cycle frequencies can easily be estimated prior to the execution of a TDOA-estimation algorithm that requires knowledge of α. Specifically, all cycle frequencies of all received signals can be estimated by simply seeking spectral lines in the FFT's of one or more lag-product waveforms $z_\tau(t) = x(t - \tau)x^*(t)$ corresponding to one or more lag values τ [1]. (Also, one can do a least squares fit over τ of $z_\tau(t)$ to $e^{i2\pi\alpha t}$ for all α of potential interest.) This capability is demonstrated in [19], where it is used in conjunction with high-resolution array-based algorithms that exploit cyclostationarity to obtain signal selectivity for direction finding. Also, the sensitivity of the performance of the TDOA-estimation methods introduced in this paper to errors in α is quantitatively evaluated in part II [1].

In the next section, we use these SNOI-free relations (43)–(45) to design a number of algorithms for estimating the TDOA with tolerance to SNOI.

IV. Cyclostationarity-Exploiting Methods for TDOA Estimation

A. Conventional GCC Methods

The conventional cross-correlation method for TDOA estimation is based on (43a) with $\alpha = 0$, which applies only in the absence of SNOI. Let us denote this idealized measurement by

$$a_0(\tau) \triangleq R_{yx}^0(\tau) = AR_s^0(\tau - D). \quad (46)$$

Since the limit autocorrelation $R_s^0(u)$ peaks at $u = 0$ for all signals, then $a_0(\tau)$ peaks at the TDOA $\tau = D$. Thus, the value of τ at which an estimate (obtained from finite time averaging) of the ideal $a_0(\tau)$ peaks can be taken as an estimate of D.

Conventional generalized cross-correlation methods for

TDOA estimation can be based on (44a)–(44c) with $\alpha = 0$, which applies only in the absence of SNOI:

$$S^0_{yx}(f) = AS^0_s(f)e^{-i2\pi fD} \tag{47a}$$

$$S^0_x(f) = S^0_s(f) \tag{47b}$$

$$S^0_y(f) = |A|^2 S^0_s(f). \tag{47c}$$

For example, if the support band of $S^0_s(f)$ is as follows:

$$S^0_s(f) = \begin{cases} > 0, & ||f| - f_0| < B_0/2 \\ = 0, & \text{otherwise} \end{cases}$$

then the ratio of (ideal) measured spectra is simply

$$\frac{S^0_{yx}(f)}{S^0_x(f)} = \begin{cases} Ae^{-i2\pi fD}, & ||f| - f_0| < B_0/2 \\ 0, & \text{otherwise} \end{cases}$$

(where the value zero is assigned by the TDOA estimation method since there is no relevant information in this ratio outside the support band and $0/0$ is undefined). Inverse Fourier transforming this ratio of spectra yields the idealized measurement

$$b_0(\tau) \triangleq \int_{||f|-f_0|<B_0/2} \frac{S^0_{yx}(f)}{S^0_x(f)} e^{i2\pi f\tau}\, df \tag{48a}$$

$$= \frac{A \sin[\pi B_0(\tau - D)]}{\pi(\tau - D)/2} \cos[2\pi f_0(\tau - D)] \tag{48b}$$

which peaks at $\tau = D$, as desired. Because of the weighting of the cross-spectrum $S^0_{yx}(f)$ by

$$W(f) \triangleq \begin{cases} \dfrac{1}{S^0_x(f)}, & ||f| - f_0| < B_0/2 \\ 0, & \text{otherwise} \end{cases}$$

the TDOA-estimation method based on an estimate of $b_0(\tau)$ is called a generalized cross-correlation (GCC) method. With $W(f) \equiv 1$, it reduces to the cross-correlation method based on an estimate of $a_0(\tau)$. Other GCC methods simply use other weighting functions $W(f)$, typically chosen to minimize the effects of noise and SNOI as revealed in (39), (40) [2], [11], [16]. However, since the use of any weighting function $W(f)$ can always be reinterpreted as simply applying the crosscorrelation method based on an estimate of $a_0(\tau)$ to spectrally filtered data $x(t)$ and $y(t)$, then whenever some SNOI cover the same spectral band as the SOI, there is little that GCC methods can do to reduce the undesirable effects of those SNOI.

B. CCC Method

To circumvent this interference problem with the GCC method, the cyclic counterpart of the conventional method based on an estimate of $a_0(\tau)$ in (46), which is called the cyclic cross-correlation (CCC) method,[3] uses an estimate of the idealized measurement from (43a)

$$a_\alpha(\tau) \triangleq |R^\alpha_{yx}(\tau)| = |A|\,|R^\alpha_s(\tau - D)| \tag{49}$$

which is valid even in the presence of SNOI. Although the peak of $|R^\alpha_s(u)|$ does not occur at $u = 0$ for all signals, since $|R^\alpha_s(u)|$ is an even function of u, there is typically a pair of peaks straddling $u = 0$ as demonstrated in Fig. 1(a) for the binary PSK (BPSK) signal with rectangular keying envelope, cycle frequency α equal to the keying rate α_k, and TDOA $D = 48T_s$, as described in the Appendix. This pair of peaks appears in the envelope of a function that oscillates with frequency equal to the carrier frequency of the signal. Thus, the midpoint of the pair of peaks in the estimate $\hat{a}_\alpha(\tau)$ of $a_\alpha(\tau)$ can be taken as an interference-tolerant estimate of the TDOA D.

As an alternative, the estimated CCC function $\hat{R}^\alpha_{yx}(\tau)$ can be correlated with its idealized version evaluated at $D = 0$, namely, $R^\alpha_s(\tau)$, and a maximum can then be sought:

$$\hat{D} \triangleq \arg\max_\tau \{\hat{a}'_\alpha(\tau)\} \tag{50}$$

where

$$\hat{a}'_\alpha(\tau) \triangleq |\hat{R}^\alpha_{yx}(\tau) \circledast R^\alpha_s(\tau)|$$

$$= \left| \int \hat{R}^\alpha_{yx}(\tau + u) R^\alpha_s(u)^*\, du \right| \tag{51}$$

where $\circledast$ denotes correlation. We refer to this alternative (50)–(51) as the correlated CCC (CCCC) method. By substituting (43a) into (51), we obtain the ideal CCCC function

$$a'_\alpha(\tau) = |A|\,|R^\alpha_s(\tau + D) \circledast R^\alpha_s(\tau)|. \tag{52}$$

A graph of this ideal CCCC function for the BPSK signal specified in the Appendix with rectangular keying envelope, $\alpha = \alpha_k$, and $D = 48T_s$ is shown in Fig. 1(b), where it can be seen that there is a unique peak (in the envelope) at $\tau = D$:

$$\arg\max_\tau \{a'_\alpha(\tau)\} = D. \tag{53}$$

If the ideal cyclic autocorrelation $R^\alpha_s(\tau)$ used in (51) is not known (to within a complex factor that is independent of τ), then it can be replaced with the estimate $\hat{R}^\alpha_x(\tau)$ since $R^\alpha_x(\tau) = R^\alpha_s(\tau)$ (cf. (43b)):

$$\hat{a}''_\alpha(\tau) \triangleq |\hat{R}^\alpha_{yx}(\tau) \circledast \hat{R}^\alpha_x(\tau)|. \tag{54}$$

The ideal version $a''_\alpha(\tau)$ of this CCCC function is exactly the same (within a scale factor) as (52) and, therefore, peaks at the TDOA $\tau = D$. This CCCC method[4]

$$\hat{D} = \arg\max_\tau \{\hat{a}''_\alpha(\tau)\} \tag{55}$$

is equivalent to the solution to a least squares fitting problem as explained following the next method.

[3]The CCC method was invented by Gardner and first disclosed in the 1985 manuscript for the book [10], which appeared in 1987. However, it was also proposed in December of 1987 by Friedman *et al.* [20], who received a patent for an implementation of it in December 1989.

[4]The CCCC method (54) is equivalent to the SPECCOA method which was invented by Gardner in 1987.

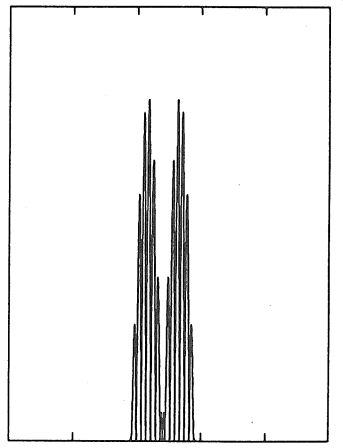

(a)

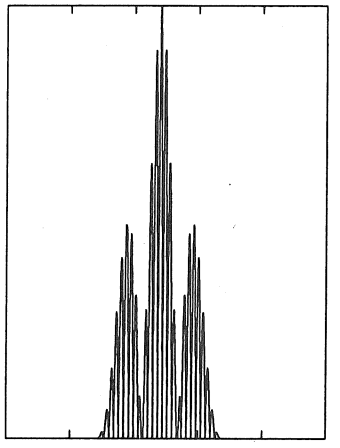

(b)

Fig. 1. (a) The ideal CCC function $a_\alpha(\tau)$ in (49) with $\alpha = \alpha_k$ for the BPSK signal with rectangular keying envelope and TDOA $D = 48T_s$. (b) The ideal CCCC function $a'_\alpha(\tau)$ in (52) with $\alpha = \alpha_k$ for the BPSK signal with rectangular keying envelope and TDOA $D = 48T_s$.

C. SPECCORR Method

The CCC method can be substantially improved on through the use of generalized CCC methods. For example, the cyclic counterpart of the GCC method based on an estimate of $b_0(\tau)$ in (48a) uses an estimate $\hat{b}_\alpha(\tau)$ of the idealized measurement

$$b_\alpha(\tau) \triangleq \left| \int_{||f|-f_\alpha|<B_\alpha/2} \frac{S_{yx}^\alpha(f)}{S_x^\alpha(f)} e^{i2\pi f\tau}\, df \right| \tag{56a}$$

$$= \left| \int_{||f|-f_\alpha|<B_\alpha/2} A e^{i2\pi f(\tau-D)}\, df \right| \tag{56b}$$

$$= |A| \left| \frac{\sin[\pi B_\alpha(\tau - D)]}{\pi(\tau - D)/2} \cos[2\pi f_\alpha(\tau - D)] \right| \tag{56c}$$

where f_α and B_α are the center and width of the support band for $S_s^\alpha(f)$ (e.g., for BPSK, if we choose $\alpha = 2f_c$, we have $f_\alpha = 0$ and $B_\alpha = B_0$; but if we choose $\alpha = \alpha_k$, we have $f_\alpha = f_c$ and $B_\alpha \cong 2\alpha_k$, see the Appendix). Like the CCCC method, this method

$$\hat{D} \triangleq \arg\max_\tau \{\hat{b}_\alpha(\tau)\} \tag{57}$$

called the spectral correlation ratio (SPECCORR) method,[5] has the advantage over the CCC method that it always produces a peak at the TDOA D (when idealized—infinite-time average—measurements are used) [9], [10]:

$$\arg\max_\tau \{b_\alpha(\tau)\} = D. \tag{58}$$

When knowledge of the parameters f_α and B_α is available, we call this the band-limited SPECCORR (BL-SPECCORR) method. On the other hand, when f_α and B_α are not available, and integration in (52a) is carried out over the entire reception band of the source location system, then the modifier BL is not used. When f_α and B_α are not known in advance, they can be selected to match the band over which the magnitude of the estimate of the ratio in the integrand in (54a) is sufficiently close to unity. Moreover, within this band, the actual magnitude can be replaced with unity to reduce undesirable random effects.

The SPECCORR method can be arrived at through a least squares optimization procedure. Specifically, since the ideal spectral correlation ratio is given by

$$\frac{S_{yx}^\alpha(f)}{S_x^\alpha(f)} = C \exp(-i[2\pi(f + \alpha/2)D - \phi]) \tag{59}$$

where $C \triangleq |A|$ and $\phi \triangleq \arg\{A\}$, then we can seek a least squares fit of $Ce^{-i[2\pi(f+\alpha/2)\tau-\phi]}$ to an estimate of the spectral correlation ratio:

$$\min_{\hat{C},\hat{\phi},\tau} \left\{ \int_{||f|-f_\alpha|<B_\alpha/2} \left| \frac{\hat{S}_{yx}^\alpha(f)}{\hat{S}_x^\alpha(f)} - \hat{C} \cdot \exp(-i[2\pi(f + \alpha/2)\tau - \hat{\phi}]) \right|^2 df \right\}. \tag{60}$$

The solution is given by

$$\hat{D} = \arg\max_\tau \{\hat{b}_\alpha(\tau)\} \tag{61}$$

where $\hat{b}_\alpha(\tau)$ is an estimate of

$$b_\alpha(\tau) \triangleq \left| \int_{||f|-f_\alpha|<B_\alpha/2} \frac{S_{yx}^\alpha(f)}{S_x^\alpha(f)} e^{i2\pi f\tau}\, df \right| \tag{62}$$

which is identical to (56a). A graph of the ideal BL-SPECCORR function (56c) for the BPSK signal described in the Appendix with $\alpha = \alpha_k$ and $D = 48T_s$ is shown in Fig. 2.

Before proceeding to discuss other generalized CCC methods, it is pointed out that unlike the GCC methods, which just use real-valued weighting functions $W(f)$ to emphasize certain spectral bands and deemphasize others,

[5]The SPECCORR method was invented by Gardner in 1986, was developed and reduced to practice jointly by Gardner and Chen, and first appeared in [10] in 1987.

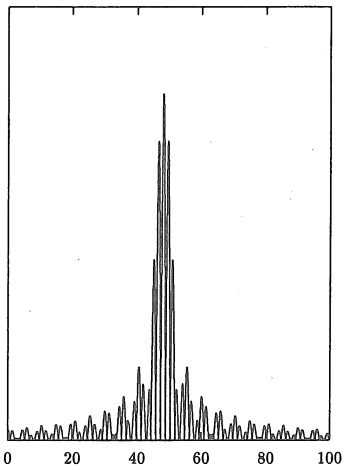

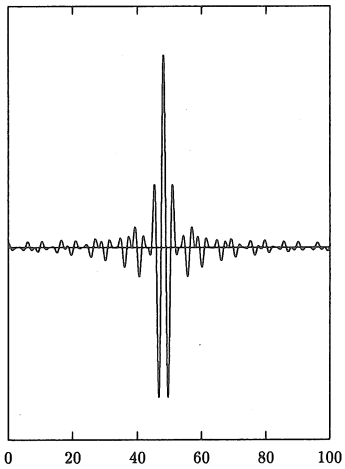

Fig. 2. (a) The ideal least squares BL-SPECCORR function $b_\alpha(\tau)$ in (56c) for complex data with $\alpha = \alpha_k$, $B_\alpha = 2\alpha_k$, and $f_\alpha = f_c$ for the BPSK signal with TDOA $D = 48T_s$. (b) The ideal least squares BL-SPECCORR function for real data with $\alpha = \alpha_k$, $B_\alpha = 2\alpha_k$, and $f_\alpha = f_c$ for the BPSK signal with TDOA $D = 47T_s$.

the weighting functions in the generalized CCC methods are complex valued and contain phase information about the SOI. Thus, they do much more than just spectral weighting in the usual sense.

D. SPECCOA Method

Other generalized CCC methods can be obtained using various ad hoc least squares optimization procedures.[6] For example, since (43a) and (43b) reveals that (ideally)

$$R^\alpha_{yx}(u) = CR^\alpha_x(u - D)e^{-i[\pi\alpha D - \phi]} \tag{63}$$

then we can seek the value of the estimate $\tau = \hat{D}$ that minimizes the sum (over the lag parameter u) of squares of error magnitudes between the measurements of the left and right sides of (63) with D replaced by τ:

$$\hat{D} \triangleq \arg\min_{\hat{C},\hat{\phi},\tau} \{\hat{c}_\alpha(\tau)\} \tag{64}$$

[6]Although classical statistical principles, such as maximum likelihood, provide an alternative approach, we have not yet found such approaches to be tractable for the non-Gaussian nonstationary models of interest.

where $\hat{c}_\alpha(\tau)$ is an estimate of

$$\begin{aligned} c_\alpha(\tau) &\triangleq \int |R^\alpha_{yx}(u) - CR^\alpha_x(u - \tau)e^{-i[\pi\alpha\tau - \phi]}|^2\, du \\ &= \int [|R^\alpha_{yx}(u)|^2 + C^2|R^\alpha_x(u - \tau)|^2 \\ &\quad - 2CRe\{R^\alpha_{yx}(u)R^\alpha_x(u - \tau)^* e^{i[\pi\alpha\tau - \phi]}\}]\, du. \end{aligned} \tag{65}$$

The solution is given by

$$\hat{D} = \arg\max_\tau \{\hat{c}'_\alpha(\tau)\} \tag{66}$$

where $\hat{c}'_\alpha(\tau)$ is an estimate of

$$\hat{c}'_\alpha(\tau) \triangleq \left| \int R^\alpha_{yx}(u)R^\alpha_x(u - \tau)^*\, du \right| \tag{67a}$$

$$= \left| \int S^\alpha_{yx}(f)S^\alpha_x(f)^* e^{i2\pi f\tau}\, df \right| \tag{67b}$$

and where (67b) follows from (67a) by using Parseval's relation for the Fourier transform. This method can be interpreted in terms of maximizing the correlation over f of two spectral correlation functions by phase alignment through adjustment of the linear phase-versus-frequency term $2\pi(f + \alpha/2)\tau$. Consequently, this approach is called the spectral coherence alignment (SPECCOA) method[7] [12]. By analogy with the SPECCORR method, it is also called the spectral correlation product (SPECCORP) method to distinguish it from SPECCORR, which also has the SPECCOA interpretation [13].

To see that $c'_\alpha(\tau)$ does indeed peak at $\tau = D$, we simply substitute (44a), (44b) into (67b) to obtain

$$c'_\alpha(\tau) = C\left| \int |S^\alpha_s(f)|^2 \exp[i2\pi(f + \alpha/2)(\tau - D)]\, df \right| \tag{68a}$$

$$\leq C\int |S^\alpha_s(f)|^2\, df \tag{68b}$$

$$= c'_\alpha(D). \tag{68c}$$

Therefore,

$$\arg\max_\tau \{c'_\alpha(\tau)\} = D. \tag{69}$$

A graph of the ideal SPECCOA function $c'_\alpha(\tau)$ given by (68a) is shown in Fig. 3 for the BPSK signal specified in the Appendix with $\alpha = \alpha_k$ and $D = 48T_s$.

An advantage of the SPECCOA function $c'_\alpha(\tau)$ over the SPECCORR function $b_\alpha(\tau)$ is that the former contains the factor $|S^\alpha_s(f)|^2$ in the integrand (cf. (68a)), whereas the latter does not (cf. (56b)). This factor can deemphasize the integrand in spectral bands where there is little contribution from the SOI, without prior knowledge of these

[7]The SPECCOA method was invented by Gardner in 1987, was developed and reduced to practice jointly by Gardner and Chen, and was first publicly disclosed at a 1988 workshop [12].

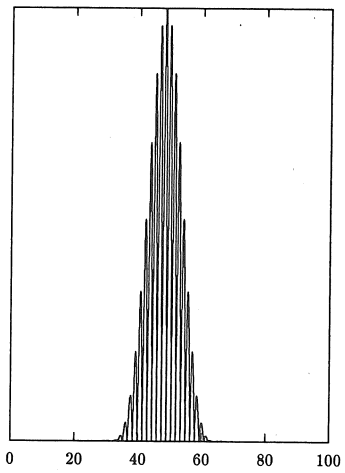

(a)

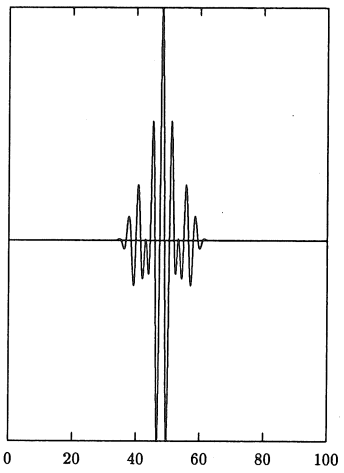

(b)

Fig. 3. (a) The ideal least squares SPECCOA function $c'_\alpha(\tau)$ in (69a) for complex data with $\alpha = \alpha_k$ for the BPSK signal with half-cosine keying envelope and TDOA $D = 48T_s$. (b) The ideal least squares SPECCOA function for real data with $\alpha = \alpha_k$ for the BPSK signal with half-cosine keying envelope and TDOA $D = 48T_s$.

bands. As the simulations in part II show, SPECCOA can indeed require less data for a MSE of the estimate $\hat{D}$ that is comparable to that of SPECCORR and even BL-SPECCORR!

It is noted that SPECCOA, as expressed in (67a) (after using the change of variables $u - \tau = v$), is identical to the ad hoc method CCCC in (54). When real-valued data is used, the scalar A in the model (38) is real and, as a result, the solutions to the least squares problems (60) and (64) with $\varphi = 0$ use the real-part operation Re $\{\cdot\}$ in place of the magnitude operation $|\cdot|$ in (62) and (67). The corresponding SPECCORR and SPECCOA functions for real data are shown in Figs. 2(b) and 3(b), respectively.

E. SPECCON Method

Another ad hoc optimization procedure is to minimize with respect to τ the sum (over the lag parameter u) of magnitude squared cyclic autocorrelation values for the difference signal $z(t) \triangleq \hat{A}x(t) - y(t + \tau)$:

$$R_z^\alpha(u) = |\hat{A}|^2 R_x^\alpha(u) + R_y^\alpha(u) e^{i2\pi\alpha\tau} - \hat{A} R_{xy}^\alpha(u - \tau) e^{i\pi\alpha\tau} - \hat{A}^* R_{yx}^\alpha(u + \tau) e^{i\pi\alpha\tau} \quad (70)$$

where, for complex data, $\hat{A}$ is complex. This is motivated by the fact that this cyclic autocorrelation would ideally be identically zero if and only if $\tau = D$ and $\hat{A} = A$, as revealed by substitution of (43a)–(43c) into (70). Since Parseval's relation yields

$$\int |R_z^\alpha(u)|^2 \, du = \int |S_z^\alpha(f)|^2 \, df \triangleq d_\alpha(\tau) \quad (71)$$

then minimization of this sum of magnitude-squared values yields the spectral coherence nulling (SPECCON) method[8]

$$\hat{D} = \arg \min_{\hat{A}, \tau} \{\hat{d}_\alpha(\tau)\} \quad (72)$$

where $\hat{d}_\alpha(\tau)$ is an estimate of $d_\alpha(\tau)$.

For applications in which $\hat{A} = 1$ is an adequate estimate, by substituting (70) into (71) and eliminating terms that are independent of τ we obtain the following equivalent TDOA estimate:

$$\hat{D} = \arg \min_{\tau} \{\hat{d}'_\alpha(\tau)\} \quad (73)$$

where $\hat{d}'_\alpha(\tau)$ is an estimate of

$$\begin{aligned} d'_\alpha(\tau) \triangleq \text{Re} \Big\{ \int & [S_x^\alpha(f) S_y^\alpha(f)^* e^{-i2\pi\alpha\tau} \\ & + S_{yx}^\alpha(f)^* S_{xy}^\alpha(f) e^{-i4\pi f\tau} \\ & - [S_x^\alpha(f)^* S_{xy}^\alpha(f) + S_y^\alpha(f) S_{yx}^\alpha(f)^*] \\ & \cdot e^{-i2\pi(f-\alpha/2)\tau} \\ & - [S_x^\alpha(f) S_{yx}^\alpha(f)^* + S_y^\alpha(f)^* S_{xy}^\alpha(f)] \\ & \cdot e^{-i2\pi(f+\alpha/2)\tau}] \, df \Big\}. \end{aligned} \quad (74)$$

By substituting (44a)–(44c) with $A = 1$ into (74), we obtain the ideal SPECCON function

$$\begin{aligned} d'_\alpha(\tau) = \text{Re} \Big\{ \int |S_s^\alpha(f)|^2 & [e^{-i2\pi\alpha(\tau - D)} + e^{-i4\pi f(\tau - D)} \\ & - 2e^{-i2\pi(f-\alpha/2)(\tau - D)} - 2e^{-i2\pi(f+\alpha/2)(\tau - D)}] \, df \Big\}. \end{aligned} \quad (75)$$

A graph of this function for the BPSK signal specified in the Appendix with $\alpha = \alpha_k$ and $D = 48T_s$ is shown in Fig. 4(a). For this BPSK signal, it can be seen that $d'_\alpha(\tau)$ not only exhibits a global minimum at $\tau = D$, but also exhibits local minima on both sides of D. For finite-time averaging, the actual global minimum can occur at one of the locations of the ideal local minima. Because these local minima are symmetric about the ideal global minimum, a pattern recognition technique can overcome the problem of choosing the wrong minimal point for the

[8]The SPECCON method was invented by Gardner in 1988, was developed and reduced to practice jointly by Gardner and Chen, and was first disclosed by Chen in [21].

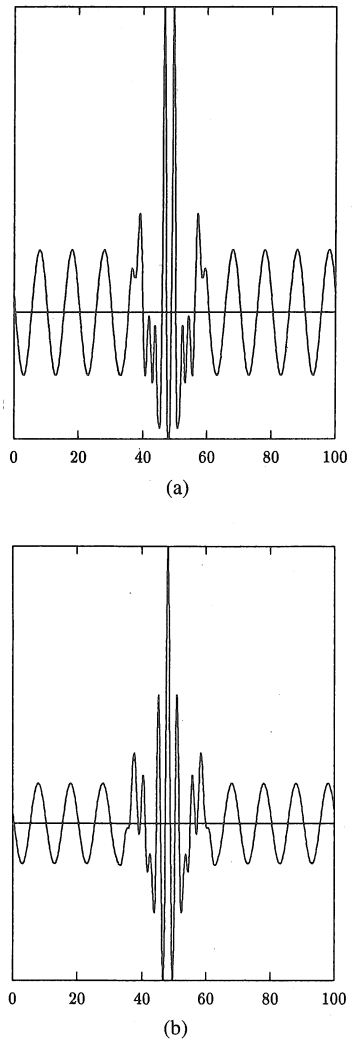

Fig. 4. (a) The ideal SPECCON function $d'_\alpha(\tau)$ in (75) with $\alpha = \alpha_k$ for the BPSK signal with half-cosine keying envelope and TDOA $D = 48T_s$. (b) The ideal PP-SPECCON function $d''_\alpha(\tau)$ corresponding to (76) (using (75) in place of $\hat{d}'_\alpha(\tau)$) with $\alpha = \alpha_k$ for the BPSK signal with half-cosine keying envelope and TDOA $D = 48T_s$.

TDOA estimate $\hat{D}$. Another approach is to circumvent the multiple minima by correlating the estimated SPECCON function $\hat{d}'_\alpha(\tau)$ with the ideal function $d'_\alpha(\tau)$ evaluated at $D = 0$ and truncated to the interval $|\tau| < 1/2\alpha_k$ (to remove excessive oscillation), and then seeking a maximum with respect to τ. A graph of the ideal version (with $d'_\alpha(\tau)$ used in place of $\hat{d}'_\alpha(\tau)$) of this postprocessed SPECCON (PP-SPECCON) function

$$\hat{d}''_\alpha(\tau) \triangleq \hat{d}'_\alpha(\tau) \circledast \bar{d}'_\alpha(\tau) \tag{76a}$$

where

$$\bar{d}'_\alpha(\tau) = \begin{cases} [d'_\alpha(\tau)]_{D=0} & |\tau| \le 1/2\alpha_k \\ 0, & |\tau| > 1/2\alpha_k \end{cases} \tag{76b}$$

is shown in Fig. 4(b) for the BPSK signal with $\alpha = \alpha_k$ and $D = 48T_s$. It can be seen that it exhibits a unique peak at $\tau = D$, as desired.

Although the simulations presented in part II for $A = 1$ show that the SPECCON method (73), without pattern recognition, performs comparably to the BL-SPECCORR method, they also show that the PP-SPECCON method

$$\hat{D} = \arg \max_\tau \{\hat{d}''_\alpha(\tau)\} \tag{77}$$

performs substantially better than even the SPECCOA method in that it yields comparable MSE with less data. Nevertheless, it does require knowledge of the ideal spectral correlation magnitude function $|S_s^\alpha(f)|$ for the SOI, whereas SPECCOA does not require any knowledge about the SOI, except of course a cycle frequency α. Also, the amount of computation required by SPECCON (even without postprocessing) is about six times that required by SPECCOA. Moreover, this simplified version of SPECCON and the corresponding PP-SPECCON are not appropriate when A in (38b) is not close to unity.

Although one might expect a postprocessed version of SPECCOA, analogous to (76), to outperform SPECCOA, this has not been found to be the case in any of the simulations performed for a BPSK SOI.

If the ideal spectral correlation magnitude $|S_s^\alpha(f)|$ used in (75)–(77) is not known (to within a factor that is independent of f), then it can be replaced with the estimate $|\hat{S}_x^\alpha(f)|$ (cf. (44b)) in (75) to obtain

$$\hat{d}'''_\alpha(\tau) \triangleq \hat{d}'_\alpha(\tau) \circledast \hat{\bar{d}}'_\alpha(\tau) \tag{78}$$

where $\hat{d}'_\alpha(\tau)$ is an estimate of (74) and $\hat{\bar{d}}'_\alpha(\tau)$ is the estimate

$$\hat{\bar{d}}'_\alpha(\tau) \triangleq \begin{cases} \operatorname{Re}\left\{ \int |\hat{S}_x^\alpha(f)|^2 [e^{-i2\pi\alpha\tau} + e^{-i4\pi f\tau} \right. \\ \left. \quad - 2e^{-i2\pi(f-\alpha/2)\tau} - 2e^{-i2\pi(f+\alpha/2)\tau}]\, df \right\}, \\ \qquad |\tau| \le 1/2\alpha_k \\ 0, \qquad |\tau| > 1/2\alpha_k. \end{cases} \tag{79}$$

F. CLP Method

Since both SPECCORR and SPECCOA methods can be interpreted in terms of indirectly estimating the slope D of the linear phase-versus-frequency characteristic displayed by their integrands, a natural alternative is to directly estimate this slope by doing a linear least squares fit to the phase data of either the ratio or conjugate product of $S_{yx}^\alpha(f)$ and $S_x^\alpha(f)$. In both cases, this phase

$$\Phi(f) \triangleq \arg\left\{\frac{S_{yx}^\alpha(f)}{S_x^\alpha(f)}\right\} \equiv \arg\{S_{yx}^\alpha(f) S_x^\alpha(f)^*\} \tag{80}$$

is given by (cf. (44a), (44b))

$$\Phi(f) = \phi - 2\pi(f + \alpha/2)D. \tag{81}$$

Thus, we want to fit the line $\hat{\phi} - 2\pi(f + \alpha/2)\hat{D}$ (with intercept $f = \hat{\phi}/2\pi\hat{D} - \alpha/2$ and slope $-2\pi\hat{D}$) to the measured phase data $\hat{\Phi}(f)$. However, without prior knowledge of $|S_s^\alpha(f)|$, we do not know which band(s) of frequencies over which to make this fit. Nevertheless,

since the spectral autocoherence magnitude

$$|C_x^\alpha(f)|^2 = \frac{|S_s^\alpha(f)|^2}{[S_s^0(f+\alpha/2) + S_n^0(f+\alpha/2)][S_s^0(f-\alpha/2) + S_n^0(f-\alpha/2)]} \tag{82}$$

is close to unity (cf. Appendix) in bands that are relatively clean ($S_s^0(f \pm \alpha/2) >> S_n^0(f \pm \alpha/2)$) and is much smaller than unity in highly corrupted bands ($S_s^0(f \pm \alpha/2) << S_n^0(f \pm \alpha/2)$), then we can use an estimate of this function as a weighting function $W(f) = |\hat{C}_x^\alpha(f)|^2$ to perform a weighted least squares fit to the phase data:

$$\min_{\hat{\phi},\tau} \left\{ \int |\hat{\Phi}(f) - \hat{\phi} + 2\pi(f+\alpha/2)\tau|^2 W(f)\, df \right\}. \tag{83}$$

The solution to this cyclic linear phase (CLP) method is given by

$$\hat{D} = \frac{-1}{2\pi} \frac{\int \bar{\hat{\Phi}}(f)\,[\bar{f}]\, W(f)\, df}{\int [\bar{f}]^2 W(f)\, df} \tag{84a}$$

where

$$\bar{\hat{\Phi}} \triangleq \hat{\Phi}(f) - \frac{\int \hat{\Phi}(f) W(f)\, df}{\int W(f)\, df} \tag{84b}$$

$$[f] \triangleq f - \frac{\int f W(f)\, df}{\int W(f)\, df}. \tag{84c}$$

In some cases, the performance of the CLP method can be improved by discarding outliers in the phase data $\hat{\Phi}(f)$ that are discovered after the fit has been made, and then refitting by reusing (84) with the expurgated phase data. Also, the numerator alone in (27) can, in some cases, be a better weighting function $W(f)$ since the corruption in an estimate of (80) that the denominator of (27) attenuates eventually becomes negligible as the data collection time grows.[9]

G. CPD Method

All methods of TDOA estimation presented up to this point are based primarily on the cross correlation or cross-spectrum properties (43a) or (44a). But the autocorrelation and autospectrum properties (43b)–(43c) and (44b)–(44c) also can be used as a basis for TDOA estimation since the phase difference for either the two cyclic autocorrelations (43b) and (43c) or the two cyclic autospectral densities (44b) and (44c) is simply $\theta_{yx} = 2\pi\alpha D$. Thus, as long as this phase difference does not exceed π in magnitude, which requires that the TDOA D, not exceed $1/2\alpha$ in magnitude, then an estimate $\hat{D}$ of that TDOA can be obtained from an estimate $\hat{\theta}_{yx}$ of the phase difference simply by dividing by $2\pi\alpha$. In many practical applications, for example, those where the two antenna elements are on two separate platforms, $|D|$ will greatly exceed $1/2\alpha$. Since we can only determine D modulo $1/\alpha$, then this phase-difference method will result in an ambiguity in the TDOA estimate except in applications where the two antenna elements are on a single platform and are sufficiently close together that $|D| < 1/2\alpha$. However, in some situations such ambiguities can be removed by other techniques, e.g., using frequency difference of arrival for moving platforms or moving signal sources, or using TDOA at different times for moving platforms.

Paralleling the derivation (65)–(66) of the SPECCOA method, we can exploit the phase-difference property

$$R_y^\alpha(u) = C^2 R_x^\alpha(u) e^{-i2\pi\alpha D} \tag{85}$$

where $C^2 = |A|^2$, over a range of lag values u by seeking the value of the estimates $\tau = \hat{D}$ and $\hat{C}$ that minimize the sum of squares of error magnitudes between the measurements of the left and right sides of (85) with D replaced by τ:

$$\hat{D} = \arg\min_{\hat{C},\tau} \{\hat{e}_\alpha(\tau)\} \tag{86}$$

where $\hat{e}_\alpha(\tau)$ is an estimate of

$$e_\alpha(\tau) \triangleq \int |R_y^\alpha(u) - C^2 R_x^\alpha(u) e^{-i2\pi\alpha\tau}|^2\, du. \tag{87}$$

The result is given explicitly by

$$\hat{D} = \frac{1}{2\pi\alpha} \text{angle} \left\{ \int \hat{R}_y^\alpha(u) \hat{R}_x^\alpha(u)^*\, du \right\} \tag{88a}$$

$$= \frac{1}{2\pi\alpha} \text{angle} \left\{ \int \hat{S}_y^\alpha(f) \hat{S}_x^\alpha(f)^*\, df \right\} \tag{88b}$$

and is referred to as the cyclic phase-difference (CPD) method.[10]

Unlike the CCCC, SPECCORR, SPECCOA, SPECCON, and CLP methods preceding this CPD method, all of which provide genuine time-difference estimates, the CPD method provides phase-difference estimates only. That is, it regenerates sine waves at each of the sensors (by forming the lag products $x(t + u/2)x(t - u/2)$ and $y(t + u/2)y(t - u/2)$), then measures their magnitudes and phases (by averaging the product of each of the lag

[9]The CLP method without weighting was first proposed by Chen in [21], and the development and reduction to practice including the incorporation of weighting functions, was carried out jointly by Gardner, Chen, and M. F. Kahn.

[10]The CPD method was invented by Gardner and first disclosed in a 1989 report for a classified research project. It was reduced to practice jointly by Gardner and C. M. Spooner and is being publicly disclosed for the first time in this paper.

products with the complex sine wave $\exp(-i2\pi\alpha t)$ to obtain $R_y^\alpha(u)$ and $R_x^\alpha(u)$), then averages the conjugate products $R_y^\alpha(u)R_x^\alpha(u)^*$ of these complex quantities, each product of which ideally has the same phase $2\pi\alpha D$, and, finally, extracts the resultant phase of this average. In fact, it can be shown that the CPD method can be interpreted as a phase interferometry method since the same estimate (88) results from nulling out the regenerated sine wave in the difference of lag products by minimizing the sum of squared magnitudes of the Fourier coefficients of the lag-product difference with respect to an adjustable time-difference (or, effectively, phase-difference) parameter τ:

$$\hat{D} = \arg\min_{\tau} \{\hat{f}_\alpha(\tau)\} \tag{89}$$

where

$$\hat{f}_\alpha(\tau) \triangleq \int |\langle [C^2 x(t - \tau + u/2)x(t - \tau - u/2) - y(t + u/2)y(t - u/2)]e^{-i2\pi\alpha t}\rangle|^2 \, du \tag{90}$$

in which $\langle \cdot \rangle$ is a finite-time average. In comparison, the SPECCON method nulls the sum of squared magnitudes of the Fourier coefficients (71) of the lag products of the difference signals $x(t) - y(t + \tau)$ with respect to an adjustable time-difference parameter τ. Thus, the SPECCON method forms difference signals, one member of which contains an adjustable delay parameter, before sine-wave regeneration, whereas the CPD method forms difference signals, one member of which contains an adjustable delay, after sine-wave regeneration.

H. Generalization to More Than Two Receivers[11]

When more than two receivers corresponding to multiple reception platforms and/or multiple antenna elements on a single platform are available, each distinct pair of receivers can be used to obtain a distinct estimate of TDOA. If there are N receivers, then there are $M = (N - 1)N/2$ distinct receiver pairs. If the distance between the antenna elements for the mth pair is L_m and the broadside angle of the mth pair with respect to an arbitrarily given direction is θ_m, then the TDOA D_m resulting from a far-field signal with a linear wavefront arriving from angle θ relative to the same given direction is

$$D_m = \frac{L_m}{c} \sin(\theta - \theta_m). \tag{91}$$

Consequently, the M TDOA estimates $\hat{D}_m$ obtained by any method(s) can be combined to obtain a single AOA estimate $\hat{\theta}$ as follows:

$$\hat{\theta} = \pm \left\langle \sin^{-1}\left(\frac{c\hat{D}_m}{L_m}\right) \mp \theta_m \right\rangle \tag{92}$$

where $\langle \cdot \rangle$ denotes average over $m = 1, 2, \cdots, M$. Of course, if some of the M individual AOA estimates are expected to be more accurate (e.g., because the corresponding distance between antenna elements is larger), then these can be weighted more heavily in a weighted average over m.

In order to remove the ambiguities (due to $\pm$) in (92), a clustering technique can be applied to the set of $2M$ estimates produced by (92) to select the appropriate M estimates (i.e., to remove the ambiguities) prior to averaging. It should be noted that when some sensor pairs have especially large separations, all other pairs should probably be omitted since their TDOA estimates will (all else being equal) be considerably less accurate. When the far-field assumption of linear wavefronts is violated, as it often is for widely separated platforms, the following alternative method can be used. This alternative also avoids the need for clustering to remove ambiguity.

Although the objective in this paper is to introduce new methods for TDOA estimation, which is usually viewed as an alternative to the high-resolution direction-finding approach based on antenna arrays with closely spaced elements (e.g., fraction-of-a-wavelength spacing), it should be mentioned that there is some potential for deriving new array-based methods from TDOA methods. This is especially evident for the CPD method since it is actually a phase-difference method. In fact, the least squares approach that led us to the CPD algorithm can be generalized from $N = 2$ to $N > 2$, and the resultant algorithm[12] shows some promise for high-resolution signal-selective source location. But, as explained above, the CPD method is, like other array-based methods, restricted to closely spaced sensors if ambiguities are to be avoided. In contrast to this, some of the TDOA methods described in this paper can be generalized from sensor pairs to sensor arrays (multiple sensor pairs or platform pairs) and there is no restriction on sensor separation for these methods. Moreover, unlike typical array-based methods, which are designed for narrow-band signals, the TDOA-based methods apply directly to wide-band signals as well as narrow-band signals. There are two approaches to accomplishing this generalization. The first approach is to produce separate TDOA estimates and then combine them to obtain a single AOA estimate as in (92). The second approach combines cyclic correlation or cyclic spectrum measurements for multiple sensor pairs and uses these jointly and directly to estimate a single AOA. Since all measurements are used jointly in a single optimization in the second approach, whereas subsets of measurements are used individually in each of multiple optimizations in the first approach, the second approach is expected to yield superior methods. Nevertheless, preliminary simulations suggest that even these superior TDOA-based methods will be inferior to high-resolution direction-finding methods when they are applicable, that is, when the sensors are separated by only fractions of a wavelength.

[11]All TDOA-based methods for AOA estimation using multiple pairs of sensors that are presented in this subsection were invented by Gardner and reduced to practice jointly by Gardner and C. M. Spooner and are being publicly disclosed for the first time in this paper.

[12]This cyclic-phase algorithm was first described by Xu and Kailath [22], and is put in perspective relative to other cyclostationarity-exploiting array-based methods in [7].

As one example of the multiple sensor-pair methods, the least squares SPECCORR method generalizes from (61) to the M-SPECCORR method[13]

$$\hat{\theta} = \arg\max_{\theta} \left\{ \sum_{m=1}^{N} \hat{b}_{\alpha}^{m\prime} \left(\frac{L_m}{c} \sin [\theta - \theta_m] \right) \right\} \quad (93)$$

where $\hat{b}_{\alpha}^{m\prime}(\tau)$ is an estimate of $\hat{b}_{\alpha}'(\tau)$ for the mth pair of sensors which produce the received signals $x_m(t)$ and $y_m(t)$ in place of $x(t)$ and $y(t)$ in (62).

Similarly, the least squares SPECCOA method generalizes from (66) to the M-SPECCOA method (assuming real data)

$$\hat{\theta} = \arg\max_{\theta} \left\{ \sum_{m=1}^{M} \hat{c}_{\alpha}^{m\prime} \left(\frac{L_m}{c} \sin [\theta - \theta_m] \right) \right\} \quad (94)$$

where $\hat{c}_{\alpha}^{m\prime}(\tau)$ is an estimate of $\hat{c}_{\alpha}'(\tau)$ for the mth pair of sensors.

When the separation between sensors is large (e.g., when the sensors are on separate platforms), the assumption of plane-wave (far-field) reception can break down, and the unique relationship (91) between $\pm$AOA and TDOA can fail to hold. In this case the hyperbolic relationship between all source locations (AOA and range) that give rise to a specific TDOA must be used in place of (91). If the two sensors in the mth pair have ranges of r_1 and r_2 and angles of θ_1 and θ_2 relative to an arbitrarily given reference point, and if the source has range r and angle θ, relative to this same reference point then we have

$$\begin{aligned} D_m = \pm \frac{1}{c} \big| & [(r_1 \cos \theta_1 - r \cos \theta)^2 \\ & + (r_1 \sin \theta_1 - r \sin \theta)^2]^{1/2} \\ & - [(r_2 \cos \theta_2 - r \cos \theta)^2 \\ & + (r_2 \sin \theta_2 - r \sin \theta)^2]^{1/2} \big| \end{aligned} \quad (95)$$

where c is the speed of propagation and D_m is the TDOA. The loci of all range/angle pairs (r, θ) that satisfy (95) for each TDOA D_m is a hyperbola. If the $\pm$ sign in (95) is known by virtue of the orientation of the sensor pair, then we can simply substitute (95) with the appropriate sign in place of $D_m = (L_m/c) \sin (\theta - \theta_m)$ in the M-SPECCORR or M-SPECCOA algorithms and replace the univariate search over θ with a bivariate search over r and θ, and thereby estimate both range and AOA. It is pointed out that this joint optimization approach to emitter location should be contrasted with the conventional approach in which individual TDOA's are estimated and the corresponding hyperbolic loci of range/angle pairs are intersected to remove ambiguity and determine a unique emitter location.

In closing this section, it is pointed out that the performance of all TDOA methods presented here can be degraded in the unusual situation where more than one spectrally overlapping signal with the *same* cycle frequency α is received. (This occurs, for example, in a multiuser code-division-multiplexed communication system.) However, the CCC method based on (49), CCCC method based on (51) (and that based on (54)), and the SPECCOA method based on (67) can operate properly when there are multiple independent identically distributed (except for a complex scale factor and time of arrival) spectrally overlapping SOI with the same α provided that their TDOAs are resolvable (cf. Section I). Moreover, the CCC method can operate properly even if the multiple signals are not identically distributed. Also, the generalization of the CPD method to $N > 2$ sensors and the other cyclostationarity-exploiting array-based methods [7] can operate properly provided that the number of signals with cycle frequency α is less than N.

[13]As an alternative, the sum in (93) can be replaced with a product.

V. Conclusion

We have introduced a new class of methods for signal-selective TDOA estimation. By exploiting the cyclostationarity property of the signal of interest, as reflected in the spectral correlation functions for the received data, the effects of additive noise and interfering signals are ideally (for unlimited data collection times) removed by these methods. As shown in part II [1] of this two-part paper, these methods can be highly tolerant to noise and interference for finite data-collection times. The signal selectivity of these methods makes it possible to apply them to closely space as well as widely separated sensors and to generalize them to multiple sensor pairs, including multiple platforms and possibly arrays of closely spaced sensors. Since their principles of operation are independent of signal bandwidth (assuming that the propagation channel and sensor characteristics are either matched or are independent of frequency throughout the signal band), these methods apply to both narrow-band and wide-band signals. Given this general applicability, it can be seen that the new class of methods at least partially bridges the gap between the previously dichotomous array-based direction finding problem and the time-difference location problem.

Appendix
The BPSK Signal[14]

A BPSK signal can be modeled by

$$s(t) = a(t) \cos (2\pi f_c t + \phi_0) \quad (A1)$$

where

$$a(t) = \sum_{n=-\infty}^{\infty} a_n q(t - t_0 - nT_k) \quad (A2)$$

in which $q(t)$ is a finite-energy keying envelope with peak height of unity and width of $T_k = 1/\alpha_k$, and $\{a_n\}$ is a binary (± 1) sequence. If $\{a_n\}$ is modeled as a sequence of independent variables with equiprobable values, then

[14]This Appendix is an abbreviation of the more complete treatment given in [10].

it can be shown that the spectral correlation function is given by

$$S_s^\alpha(f) = \frac{1}{4T_k}\left[Q\left(f + f_0 + \frac{\alpha}{2}\right)Q^*\left(f + f_0 - \frac{\alpha}{2}\right) + Q\left(f - f_0 + \frac{\alpha}{2}\right)Q^*\left(f - f_0 - \frac{\alpha}{2}\right)\right]e^{-i2\pi\alpha t_0}$$

for $\alpha = n/T_k$ and

$$S_s^\alpha(f) = \frac{1}{4T_k}\left[Q\left(f + f_0 + \frac{\alpha}{2}\right)Q^*\left(f - f_0 - \frac{\alpha}{2}\right) \cdot e^{-i(2\pi[\alpha + 2f_c]t_0 + 2\phi_0)} + Q\left(f - f_0 + \frac{\alpha}{2}\right)Q^*\left(f + f_0 - \frac{\alpha}{2}\right) \cdot e^{-i(2\pi[\alpha - 2f_c]t_0 - 2\phi_0)}\right] \quad \text{(A3)}$$

for $\alpha = \pm 2f_c + n/T_k$ for all integers n, and $S_s^\alpha(f) \equiv 0$ for all other values of α. In (A3), $Q(f)$ is the keying envelope transform

$$Q(f) = \int_{-\infty}^{\infty} q(t)e^{-i2\pi ft}\,dt. \quad \text{(A4)}$$

The inverse Fourier transform of (A3) is given by

$$R_s^\alpha(\tau) = \int_{-\infty}^{\infty} S_s^\alpha(f)e^{i2\pi f\tau}\,df = \frac{1}{2T_k}r_q^\alpha(\tau)\cos(2\pi f_c\tau)e^{-i2\pi\alpha t_0} + \frac{1}{4T_k}[r_q^{\alpha+2f_c}(\tau)e^{-i(2\pi[\alpha+2f_c]+2\phi_0)} + r_q^{\alpha-2f_c}(\tau)e^{-i(2\pi[\alpha-2f_c]t_0-2\phi_0)}] \quad \text{(A5)}$$

where

$$r_q^\alpha(\tau) = \int_{-\infty}^{\infty} q\left(t + \frac{\tau}{2}\right)q\left(t - \frac{\tau}{2}\right)e^{-i2\pi\alpha t}\,dt \quad \text{(A6)}$$

for $\alpha = n/T_k$ for all integers n.

Graphs of the magnitudes of the functions $S_s^\alpha(f)$ and $R_s^\alpha(\tau)$ are shown in Figs. 5 and 6 for the case of a full-duty-cycle rectangular keying envelope

$$q(t) \triangleq \begin{cases} 1, & |t| \le T_k/2 \\ 0, & \text{otherwise} \end{cases} \quad \text{(A7)}$$

with keying rate $\alpha_k = 1/T_k = 1/10$ and carrier frequency $f_c = 0.33$. In these graphs the magnitudes of the complex-valued functions are plotted as the heights of surfaces above the planes with coordinates f and α. Since the functions can be nonzero for only discrete values of the cycle frequency parameter α, the surfaces consist of infinitesimally thin slices parallel to the f or τ axis.

The graphs of the TDOA functions for BPSK shown in Fig. 1 were obtained using the rectangular keying envelope, but those in Figs. 2–4 were obtained using the more practical full-duty-cycle half-cosine keying envelope:

$$q(t) \triangleq \begin{cases} \cos(\pi t/T_k), & |t| \le T_k/2 \\ 0, & \text{otherwise.} \end{cases} \quad \text{(A8)}$$

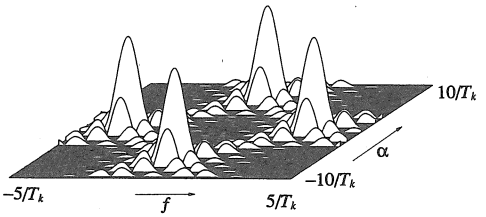

Fig. 5. Magnitude of the spectral correlation function for a BPSK signal with rectangular keying envelope and $f_c = 3.3/T_k$ and $T_k = 10$.

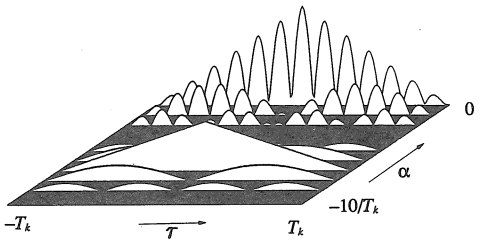

Fig. 6. Magnitude of the cyclic autocorrelation function for a BPSK signal with rectangular keying envelope and $f_c = 3.3/T_k$ and $T_k = 10$.

Acknowledgment

The authors gratefully acknowledge Dr. S. V. Schell and C. M. Spooner for their contributions to the refinement of earlier drafts of this paper and for confirming some of the analytical results.

References

[1] C. K. Chen and W. A. Gardner, "Signal-selective time-difference-of-arrival estimation for passive location of man-made signal sources in highly corruptive environments, Part II: algorithms and performance," *IEEE Trans. Signal Processing*, this issue, pp. 1185–1197.

[2] G. C. Carter, Ed., *IEEE Trans. Acoust., Speech, Signal Processing*, vol. ASSP-29, part II, June 1981.

[3] S. Stein, "Algorithms for ambiguity function processing," *IEEE Trans. Acoust., Speech, Signal Processing*, vol. ASSP-29, pp. 588–599, June 1981.

[4] A. Paulraj, R. Roy, and T. Kailath, "Estimation of signal parameters via rotational invariance techniques—ESPRIT," in *Proc. Nineteenth Asilomar Conf. Signals, Syst., Comput.* (Pacific Grove, CA), Nov. 1985.

[5] R. O. Schmidt, "A signal subspace approach to multiple source location and spectral estimation," Ph.D. dissertation, Stanford University, Stanford, CA, 1981.

[6] M. Viberg and B. Ottersten, "Sensor array processing based on subspace fitting," *IEEE Trans. Signal Processing*, vol. 39, no. 5, pp. 1122–1135, May 1991.

[7] S. V. Schell and W. A. Gardner, "High resolution direction finding," in *Handbook of Statistics*, vol. 10, N. K. Bose and C. R. Rao, Eds. Amsterdam: Elsevier, 1992.

[8] M. Viberg, B. Ottersten, and T. Kailath, "Detection and estimation in sensor arrays using weighted subspace fitting," *IEEE Trans. Acoust., Speech, Signal Processing*, vol. 39, pp. 2436–2449, Nov. 1991.

[9] I. Ziskind and M. Wax, "Maximum likelihood localization of multiple sources by alternating projections," *IEEE Trans. Acoust., Speech, Signal Processing*, vol. ASSP-36, pp. 1553–1560, Oct. 1988.

[10] W. A. Gardner, *Statistical Spectral Analysis: A Nonprobabilistic Theory*. Englewood Cliffs, NJ: Prentice-Hall, 1987.

[11] W. A. Gardner and C. K. Chen, "Interference tolerant time-difference-of-arrival estimation for modulated signals," *IEEE Trans. Acoust., Speech, Signal Processing*, vol. ASSP-36, pp. 1385–1395, Sept. 1988.
[12] W. A. Gardner and C. K. Chen, "Selective source location by exploitation of spectral coherence," in *Proc. IEEE/ASSP Fourth Workshop Spectrum Estimation Modeling* (Minneapolis, MN), Aug. 1988, pp. 271–276.
[13] W. A. Gardner, *Introduction to Random Processes with Applications to Signals and Systems*, 2nd ed. New York: McGraw-Hill, 1989.
[14] W. A. Gardner, "The spectral correlation theory of cyclostationary time-series," *Signal Processing*, vol. 11, pp. 13–36, 1986.
[15] W. A. Gardner, "Exploitation of spectral redundancy in cyclostationary signals," *IEEE Signal Processing Mag.*, vol. 8, pp. 14–36, Apr. 1991.
[16] G. C. Carter, "Coherence and time delay estimation," *Proc. IEEE*, vol. 75, pp. 236–255, Feb. 1987.
[17] W. A. Gardner, "Spectral correlation of modulated signals: Part I—Analog modulation," *IEEE Trans. Commun.*, vol. COM-35, no. 6, pp. 584–594, June 1987.
[18] W. A. Gardner, W. A. Brown, III, and C. K. Chen, "Spectral correlation of modulated signals: Part II—Digital modulation," *IEEE Trans. Commun.*, vol. COM-35, no. 6, pp. 595–601, June 1987.
[19] S. V. Schell and W. A. Gardner, "Progress on signal-selective direction finding," in *Proc. Fifth ASSP Workshop Spectrum Estimation Modeling* (Rochester, NY), Oct. 10–12, 1990, pp. 144–148.
[20] J. S. Friedman, J. P. King, and J. P. Pride, "Time difference of arrival geolocation method," U.S. Patent 4 888 593, Dec. 19, 1989.
[21] C. K. Chen, "Spectral correlation characterization of modulated signals with application to signal detection and source location," Ph.D. dissertation, Dep. Elec. Eng. Comput. Sci., Univ. California, Davis, CA, Mar. 1989.
[22] G. Xu and T. Kailath, "Direction-of-arrival estimation via exploitation of cyclostationarity—a combination of spatial and temporal processing," *IEEE Trans. Signal Processing*, to be published July 1992.
[23] W. A. Gardner, "A unifying view of coherence in signal processing," *Signal Processing*, vol. 26, 1992, to be published.

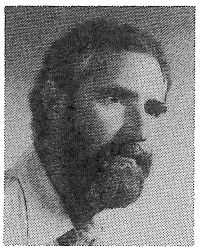

William A. Gardner (S'64–M'67–SM'84–F'91) was born in Palo Alto, CA, on November 4, 1942. He received the M.S. degree from Stanford University in 1967 and the Ph.D. degree from the University of Massachusetts, Amherst, in 1972, both in electrical engineering.

He was a Member of the Technical Staff at Bell Laboratories in Massachusetts from 1967 to 1969. He has been a faculty member at the University of California, Davis, since 1972, where he is Professor of Electrical Engineering and Computer Science. Since 1982, he has also been President of the engineering consulting firm Statistical Signal Processing, Inc., Yountville, CA. His research interests are in the general area of statistical signal processing, with primary emphasis on the theories of time-series analysis, stochastic processes, and signal detection and estimation. He is the author of *Introduction of Random Processes with Applications to Signals and Systems* (Macmillan, 1985, second edition, McGraw-Hill, 1990), *The Random Processes Tutor: A Comprehensive Solutions Manual for Independent Study* (McGraw-Hill, 1990), and *Statistical Spectral Analysis: A Nonprobabilistic Theory* (Prentice-Hall, 1987). He holds several patents and is the author of numerous research-journal papers.

Dr. Gardner received the Best Paper of the Year Award from the European Association for Signal Processing in 1986 for the paper entitled "The Spectral Correlation Theory of Cyclostationary Signals," the 1987 Distinguished Engineering Alumnus Award from the University of Massachusetts, and the Stephen O. Rice Prize Paper Award in the Field of Communication Theory from the IEEE Communications Society in 1988 for the paper entitled "Signal Interception: A Unifying Theoretical Framework for Feature Detection." He is a member of the American Mathematical Society, the American Association for the Advancement of Science, and the European Association for Signal Processing, and a member of the honor societies Sigma Xi, Tau Beta Pi, Eta Kappa Nu, and Alpha Gamma Sigma.

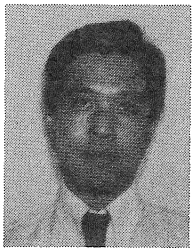

Chih-Kang Chen (S'82–M'89) received the B.S. degree from California State University, Sacramento, in 1983 and the M.S. and Ph.D. degrees from the University of California, Davis, in 1985 and 1989, respectively, all in electrical engineering.

From April 1989 to February 1990, he was a postdoctoral fellow at The University of California, Davis, performing research work in the area of signal detection and parameter estimation. Since February 1990 he has been with Silicon Engines developing fully digital real-time spectrum analyzers for NASA's Search for Extra-Terrestrial Intelligence (SETI) project. His research interests include signal detection and estimation and digital signal processing. He is the coauthor (with W. A. Gardner) of *The Random Processes Tutor: A Comprehensive Solutions Manual for Independent Study* (McGraw-Hill, 1990).